J Nanostruct 16(4): 5715-5725, Autumn 2026

RESEARCH PAPER

Plasmonic Random Lasing from Rhodamine 6G dye Gain Medium Assisted by Silver Nanowire Waveguides

***Saja. M. Yass, S. F. Haddaw** **

Department of Laser Physics, College of Science for Women, University of Babylon, Babylon, Iraq

ARTICLE INFO

Article History:
Received 29 May 2026
Accepted 26 September 2026
Published 01 October 2026

Keywords:
Optical gain
Random laser
Plasmonic
Rhodamine 6G
Silver nanowires

ABSTRACT

Plasmonic random lasers offer a promising approach to integrating optical gain, multiple light scattering, and plasmon-assisted light–matter interactions. In this study, a random-laser configuration assisted by silver nanowires (AgNWs), with Rhodamine 6G (R6G) serving as the gain medium, was experimentally examined. Initially, the optical response of R6G was evaluated at concentrations ranging from 1×10^{-6} to 5×10^{-5} M through absorption and fluorescence spectroscopy. The absorption intensity increased continuously with increasing concentration, whereas the fluorescence intensity exhibited a maximum at 1×10^{-5} M. Accordingly, this concentration was identified as the optimal condition for the gain medium. The selected R6G solution was then assessed under ten different pump-energy levels spanning 0.5–3.5 mJ. As the pump energy increased, the emission peak intensity rose from 10,610.167 to 51,353.000 a.u., representing an approximately 4.84-fold increase. Despite this substantial enhancement, the dominant emission wavelength remained within the narrow range of 566.308–566.577 nm, corresponding to a maximum spectral shift of approximately 0.27 nm. Furthermore, increasing the pump energy resulted in a reduction in the emission linewidth from 8.958 nm to a minimum full width at half maximum (FWHM) of 3.641 nm at 3.5 mJ. Over the same energy range, the peak-to-background ratio increased from 4.163 to a maximum of 5.700. Based on the emission response as a function of pump energy, the lasing threshold was established at 1.7 mJ These results indicate progressive spectral narrowing, enhanced peak-to-background contrast, and the development of pronounced stimulated emission above the threshold. The observed pump-energy-dependent emission characteristics support a hybrid gain–scattering mechanism, whereby R6G supplies optical amplification, while the Ag nanowire network provides multiple-scattering pathways and plasmon-assisted optical feedback.

How to cite this article
Yass S., Haddaw S. Plasmonic Random Lasing from Rhodamine 6G dye Gain Medium Assisted by Silver Nanowire Waveguides. J Nanostruct, 2026; 16(4):5715-5725. DOI: 10.22052/JNS.2026.04.100

INTRODUCTION

Random lasers (RLs) represent a distinctive category of laser sources in which optical feedback arises from multiple scattering processes rather than from a conventional optical resonator [1-3]. Unlike traditional lasers, these systems do not require a specifically designed pair of mirrors to sustain optical feedback, as repeated scattering events within a disordered gain medium can establish distributed feedback pathways [4, 5]. Owing to this unique operating principle, random lasers have attracted considerable research

* *Corresponding Author Email: wsci.saddem.flayeh@uobabylon.edu.iq*

This work is licensed under the Creative Commons Attribution 4.0 International License.
To view a copy of this license, visit http://creativecommons.org/licenses/by/4.0/.

interest in various fields, including photonics, sensing, imaging, and spectroscopy [6-14].

The operational characteristics of random lasers are primarily determined by the interplay between optical gain and optical feedback [15]. Among the various gain materials, organic laser dyes, particularly Rhodamine 6G (R6G), are extensively employed because of their strong absorption in the visible spectral region and high fluorescence efficiency [16]. However, increasing the dye concentration does not necessarily lead to a continuous improvement in effective optical gain [17, 18]. At higher concentrations, processes such as reabsorption and concentration-dependent molecular interactions may diminish fluorescence efficiency and influence the resulting lasing characteristics [19]. Therefore, identifying an appropriate dye concentration is a crucial preliminary step in the experimental investigation of random-laser operation [20].

Plasmonic metallic nanostructures provide an effective approach to manipulating optical fields and modifying feedback mechanisms in random-laser systems [21]. Among these structures, silver nanowires (Ag NWs) have attracted particular attention because their elongated morphology supports plasmonic modes while also enabling strong light scattering and nanoscale optical confinement [22]. As a result, Ag NWs can contribute to optical waveguiding, scattering processes, and plasmon-mediated light–matter interactions [23, 24].

The integration of silver nanowires with Rhodamine 6G (R6G)-based random lasers has been investigated in several previous studies. Sun et al. demonstrated enhanced stimulated emission from R6G in the presence of Ag nanowires and reported coherent random-laser emission at a low excitation threshold, highlighting the contribution of surface-plasmon effects [25]. Subsequently, a waveguide–plasmonic architecture incorporating R6G-doped polydimethylsiloxane (PDMS) and Ag nanowires was developed, in which the R6G/PDMS layer functioned as an active waveguide and the nanowire network provided three-dimensional plasmonic feedback [26, 27]. Further research demonstrated a mechanically tunable waveguide–plasmonic random laser based on the same combination of R6G-doped PDMS and silver nanowires [28].

Additional investigations by Haddawi and co-workers have explored plasmonic random-lasing behavior in a range of configurations, including plexcitonic structures, plasmonic nanoparticles, multilayer assemblies of Ag nanowires, and tunable nanowire-based systems [29-31]. These findings complement broader research on optical feedback in random lasers, spectral narrowing, lasing-threshold determination, plasmonic waveguides, and the photophysical properties of R6G [32]. More recent studies published in the *Journal of Theoretical and Applied Physics* have examined R6G-based plasmonic random lasers for applications such as tissue imaging, as well as temperature-dependent gain and feedback mechanisms and core–shell plasmonic nanoparticles. In related research, plasmonic meta-surfaces have also been shown to enhance dye fluorescence, further illustrating the potential of plasmonic structures to modify light–matter interactions [33-35].

Despite the progress achieved in this field, the concentration of the gain medium remains a key factor in experimental optimization. This is because maximum pump-light absorption does not necessarily correspond to the highest fluorescence output or the most favorable conditions for optical amplification. Accordingly, evaluating both absorption and fluorescence experimentally provides a reliable basis for selecting the gain-medium concentration before conducting random-laser measurements.

In this study, a random-laser system incorporating silver nanowires (Ag NWs) and Rhodamine 6G (R6G) is investigated. The concentration-dependent absorption and fluorescence responses of R6G are initially characterized across the selected concentration range. Based on the measured fluorescence spectrum, a concentration of 1×10^{-5} M is chosen because it yields the highest fluorescence intensity. Subsequently, the selected gain medium is examined under ten pump-energy conditions ranging from 0.5 and 3.5 mJ. The resulting variations in emission peak intensity, wavelength, spectral linewidth, and peak-to-background ratio are systematically evaluated to characterize the pump-energy-dependent emission behavior of the plasmonic random-laser system.

MATERIALS AND METHODS

Silver Nanowire Preparation

The Ag nanowires were synthesized following the procedure reported by Ejbarah et al. [7].

CC BY

Polydimethylsiloxane (PDMS) preparation

Polydimethylsiloxane (PDMS) was employed as the polymeric host matrix for the R6G-containing gain layer. The PDMS base was combined with the curing agent at a weight ratio of 10:1. Specifically, 0.20 g of the PDMS base was mixed with 0.02 g of the curing agent to prepare the polymer matrix. This mixing ratio was adopted in accordance with the preparation procedure reported by Haddawi et al. [8].

Sample Structure and Fabrication

The plasmonic random-laser structure was designed using three main components: a substrate, a silver nanowire (Ag NWs) layer, and an R6G-containing gain medium. Rhodamine 6G (R6G) served as the optical gain material, whereas the Ag NWs were incorporated to provide plasmonic interactions and light scattering. Accordingly, the sample architecture consisted of a substrate/Ag NW/R6G configuration. The schematic illustration of the plasmonic random-laser structure and its multilayer configuration are shown in Fig. 1a. For reproducibility, the substrate material, composition of the polymeric gain layer, Ag NW concentration, nanowire dimensions, film

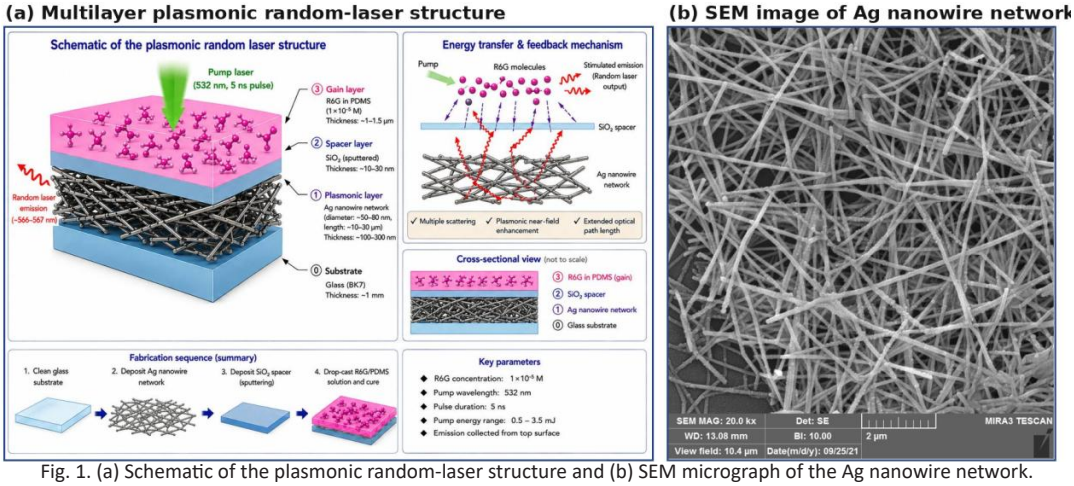


Fig. 1. (a) Schematic of the plasmonic random-laser structure and (b) SEM micrograph of the Ag nanowire network.

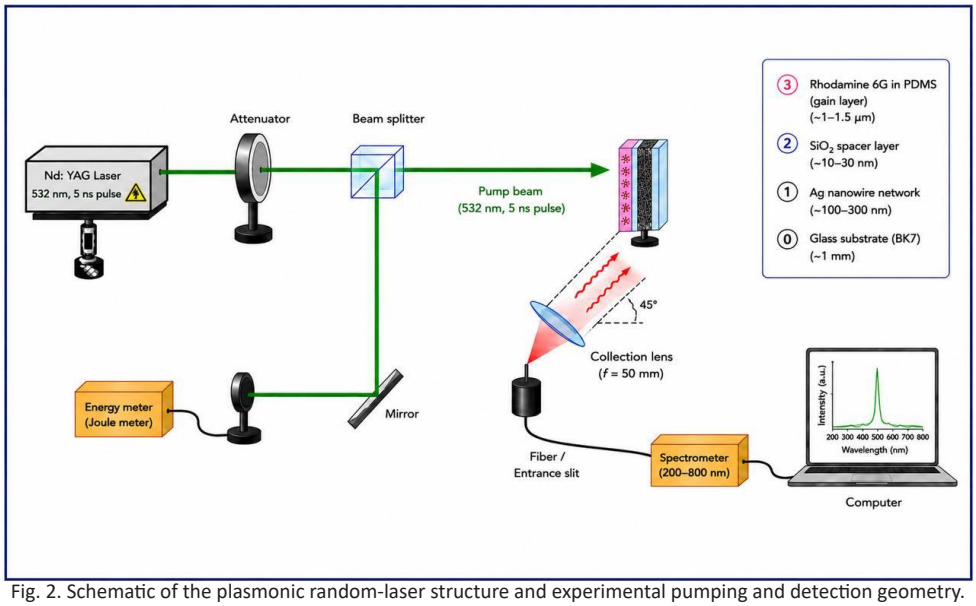


Fig. 2. Schematic of the plasmonic random-laser structure and experimental pumping and detection geometry.

CC BY

thickness, and relevant fabrication conditions are specified based on the experimental procedures used in this study.

Random-Laser Measurement Setup

The R6G/PDMS gain layer, containing R6G at an optimized concentration of (1 × 10^{-5} M) M, was excited using a pulsed laser with a wavelength of 532 nm. The emitted light was collected at an angle of 45° relative to the excitation geometry and analyzed using a spectrometer. Emission spectra were recorded at ten pump energies: 0.5, 0.8, 1.3, 1.4, 1.7, 2.1, 2.4, 2.8, 3.1, and 3.5 mJ. Fig. 2 illustrates the multilayer plasmonic random-laser structure and the experimental pumping and detection geometry.

Characterization

Morphological Characterization

Scanning electron microscopy (SEM) was used to examine the morphology and spatial distribution of the Ag nanowire network. The SEM micrograph was used to assess the nanowire arrangement and the formation of interconnected structures within the network.

Optical Characterization

Rhodamine 6G (R6G) solutions with concentrations of 1×10^{-6}, 5×10^{-6}, 1×10^{-5}, and 5×10^{-5} M were characterized using UV–Vis absorption and fluorescence spectroscopy to investigate their optical properties and identify a suitable gain-medium concentration for subsequent random-laser experiments.

RESULTS AND DISCUSSION

Morphological Analysis of the Ag Nanowire Network

Fig. 1b shows the SEM micrograph of the Ag nanowire network used in the plasmonic random-laser structure. The nanowires appear densely distributed and randomly oriented, forming numerous junctions and interconnected pathways. Such a network morphology may promote multiple light-scattering events and contribute to optical feedback within the structure. However, the contribution of the Ag NWs network to random-laser feedback should be evaluated alongside the optical emission measurements.

Absorption and Fluorescence Spectra of R6G

The UV–Vis absorption spectra of the R6G solutions exhibited an absorption maximum at approximately 530–531 nm, while the fluorescence spectra showed an emission maximum at approximately 552–553 nm. Among

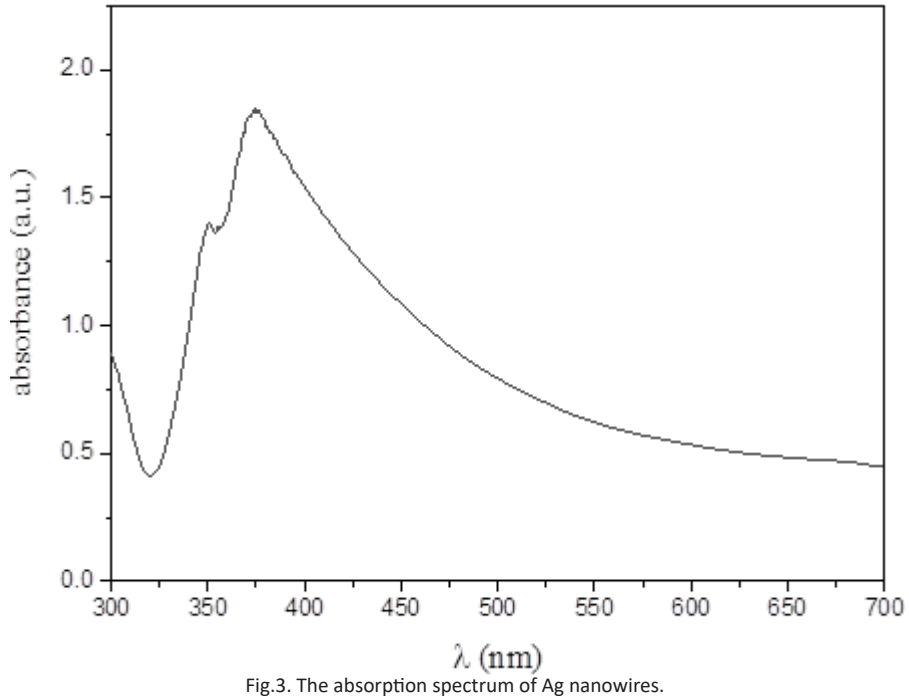


Fig.3. The absorption spectrum of Ag nanowires.

CC BY

the investigated concentrations, the solution exhibiting the highest fluorescence intensity was selected for the subsequent random-laser experiments. The concentration-dependent fluorescence response was therefore used as a criterion for selecting the R6G concentration for further measurements.

Random-Laser Emission Characteristics

The random-laser emission characteristics of the R6G/PDMS gain layer integrated with the Ag NW network were investigated by recording the emission spectra at different pump energies. The measured spectra were analyzed to evaluate the dependence of the emission intensity and spectral linewidth on the pump energy.

Absorption Spectra of Ag NWs

Fig. 3 shows the absorption spectrum of Ag nanowires dispersed in deionized water. As can be seen, the absorption spectrum of Ag nanowires exhibits two relatively sharp surface plasmon resonance (SPR) peaks. These two absorption bands correspond to the longitudinal and transverse plasmon bands. The longitudinal plasmon band is attributed to the absorption and scattering of light along the long axis of the nanowires, whereas the transverse plasmon band arises from the same processes along their short axis. The center of the longitudinal plasmon band is located at approximately 378 nm, while the center of the transverse plasmon band is located at approximately 351 nm.

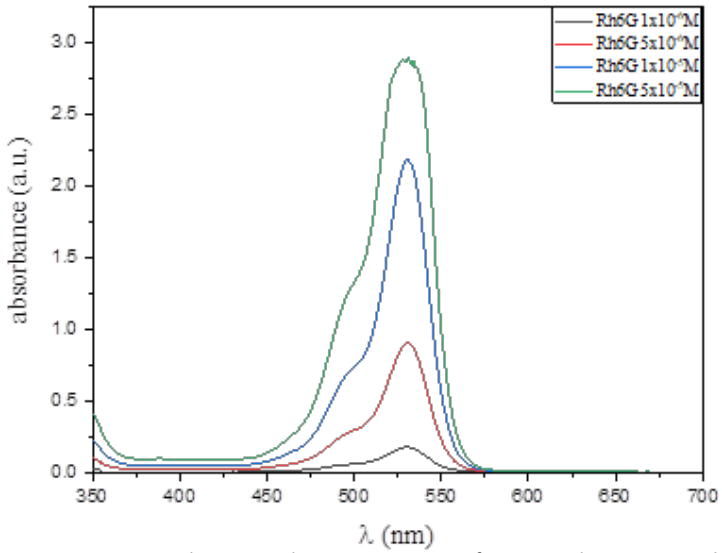


Fig. 4. Experimental UV–Vis absorption spectra of R6G at the investigated concentrations.

Table 1. Concentration-dependent absorption parameters of R6G.

R6G concentration	λmax (nm)	Maximum absorbance
1×10^{-6} M	530	0.182
5×10^{-6} M	531	0.910
1×10^{-5} M	531	2.185
5×10^{-5} M	531	2.892

CC BY

Concentration-dependent absorption of R6G

According to Fig. 4 and Table 1, the absorption spectra exhibit a pronounced absorption band in the green region of the spectrum, with a maximum at approximately 530–531 nm. As the R6G concentration increases, the absorption intensity increases, while the position of the absorption maximum remains essentially unchanged. The maximum absorbance values are approximately 0.182, 0.910, 2.185, and 2.892 at R6G concentrations of 1×10^{-6}, 5×10^{-6}, 1×10^{-5}, and 5×10^{-5} M, respectively. This monotonic increase in absorbance is consistent with the increasing number of dye molecules available to absorb pump photons. However, the concentration corresponding to the highest absorbance cannot, by itself, be considered the optimum lasing concentration, since optical gain also depends on fluorescence efficiency and loss processes.

Fluorescence Optimization of the R6G gain medium

According to Fig. 5 and Table 2, the fluorescence spectra are centered at approximately 552–553 nm. The maximum measured fluorescence intensities are approximately 10,358, 15,678, 36,013, and 23,536 counts at R6G concentrations

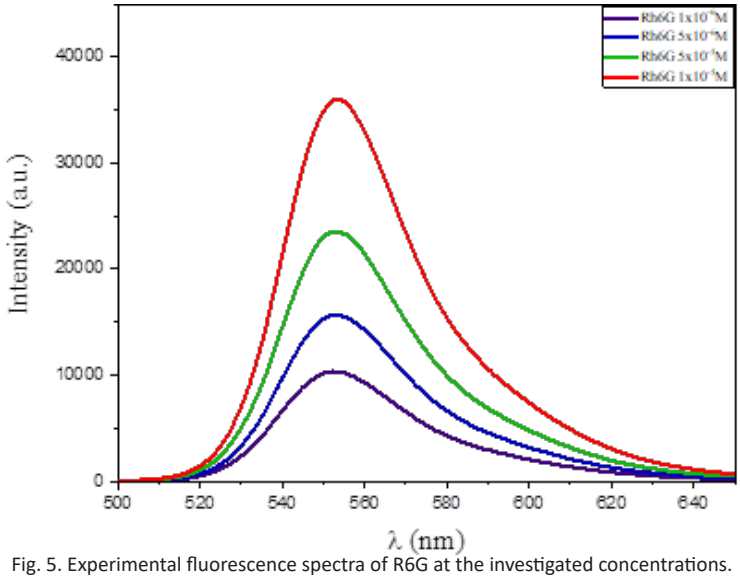


Fig. 5. Experimental fluorescence spectra of R6G at the investigated concentrations.

Table 2. Concentration-dependent fluorescence parameters of R6G.

R6G concentration	Emission peak (nm)	Maximum fluorescence intensity (counts)
1×10^{-6} M	552.400	10357.900
5×10^{-6} M	553.300	15677.500
1×10^{-5} M	553.300	36012.600
5×10^{-5} M	553.300	23536.300

CC BY

of 1×10^{-6}, 5×10^{-6}, 1×10^{-5}, and 5×10^{-5} M, respectively. Thus, the 1×10^{-5} M solution exhibits the highest fluorescence intensity among the investigated concentrations. Notably, the sample with a concentration of 5×10^{-5} M exhibits higher absorption but lower fluorescence intensity than the 1×10^{-5} M sample. Its fluorescence intensity is approximately 34.6% lower than that of the latter. This behavior indicates that stronger pump absorption does not necessarily result in stronger useful emission. The reduction in fluorescence intensity at the highest concentration may be associated with concentration-dependent loss mechanisms, such as reabsorption, aggregation, or fluorescence quenching; however, the present data do not allow these mechanisms to be distinguished independently. Accordingly, a concentration of 1×10^{-5} M was selected for the gain medium in the random-laser measurements.

Pump-Energy-Dependent Random-Laser Emission

As summarized in Table 3, the optimized R6G gain medium was investigated at ten different pump energies ranging from 0.5 to 3.5 mJ. A substantial increase in the dominant emission intensity was observed as the pump energy increased. The peak intensity increased from approximately 10,610 a.u. at 0.5 mJ to 51,353 a.u. at 3.5 mJ, corresponding to an enhancement factor of approximately 4.84, as shown in Fig. 6. This increase is consistent with stronger optical excitation and a higher population of excited R6G molecules, thereby increasing the available optical gain. In the hybrid structure, this gain is accompanied by scattering and plasmon-

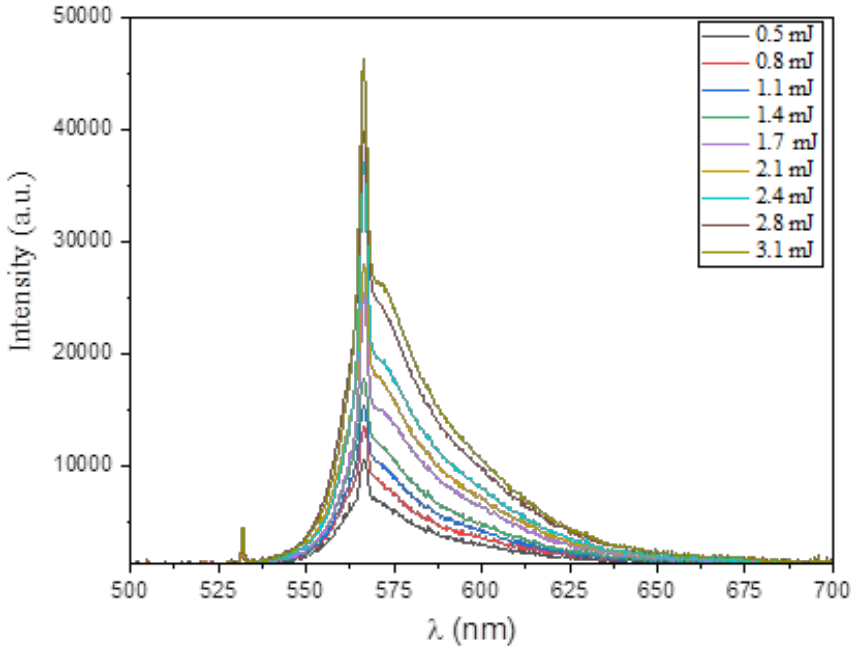


Fig. 6. Experimental random-laser emission spectra measured at ten pump energies.

Table 3. Quantitative spectral parameters of the random-laser emission.

Pump energy (mJ)	Peak wavelength (nm)	Raw peak intensity (a.u.)	FWHM (nm)	Peak/background ratio
0.5	566.577	10610.167	8.958	4.163
0.8	566.577	13602.778	8.249	4.138
1.1	566.308	15314.222	8.241	4.400
1.4	566.308	17747.000	7.287	4.180
1.7	566.577	25458.833	5.771	4.886
2.1	566.308	28015.778	5.156	5.131
2.4	566.308	37072.611	4.744	5.280
2.8	566.308	39873.722	3.971	5.386
3.1	566.308	46388.111	3.814	5.528
3.5	566.308	51353.000	3.641	5.700

CC BY

mediated interactions associated with the Ag nanowire network.

Emission-Wavelength Stability

The dominant emission peak remains centered at approximately 566–567 nm over the entire investigated pump-energy range. The peak position varies from approximately 566.31 to 566.58 nm, corresponding to a maximum shift of only about 0.27 nm. The strong stability of the emission wavelength indicates that increasing the pump energy primarily modifies the emission intensity rather than substantially shifting the dominant spectral band.

Linewidth and Peak-to-Background Evolution

As shown in Fig. 7a and b, the extracted linewidth exhibits a non-monotonic dependence on pump energy rather than a continuous decrease. The narrowest measured emission feature occurs at a pump energy of 3.5 mJ, where the full width at half maximum (FWHM) is approximately 3.641 nm and the peak-to-background ratio is approximately 5.7. The absence of monotonic linewidth narrowing indicates that the results should not be interpreted as a continuous decrease in FWHM with increasing pump energy. Instead, the findings reveal pump-energy-dependent spectral evolution, with particularly narrow emission features observed at selected excitation energies.

Interpretation of the Plasmonic Random-Lasing Mechanism

The experimental observations can be interpreted in terms of a hybrid gain–scattering mechanism. R6G molecules absorb the pump photons and provide optical gain, whereas the Ag nanowire network introduces multiple scattering pathways and plasmon-mediated electromagnetic interactions. Thus, the nanowire network acts as a distributed feedback medium rather than forming a conventional cavity defined by discrete mirrors. This interpretation is consistent with previous studies of Ag-NW/R6G random lasers, which have reported enhanced stimulated emission and plasmonic feedback associated with Ag nanowires [1-8].

The proposed mechanism can be summarized as follows: pump absorption by R6G → excitation of R6G molecules → optical gain → scattering by Ag nanowires → plasmon-assisted local-field enhancement and recurrent optical pathways → amplification of selected emission channels → narrow random-laser emission around 566–567 nm. However, attributing the observed emission exclusively to a specific Ag plasmon resonance would require further evidence, such as an independent extinction or scattering spectrum of the Ag-nanowire sample used in the experiments, or electromagnetic simulations of the hybrid system.

Random-Lasing Threshold: Experimental Limitation

The pump-energy dependence of the random-laser peak intensity is illustrated in Fig. 8. As the pump energy increased from 0.5 to 3.5 mJ, the emission intensity increased from 10,610.167 to 51,353.000 a.u. Based on the observed emission response as a function of pump energy, the random-lasing threshold was estimated to be approximately 1.7 mJ. At this energy, the

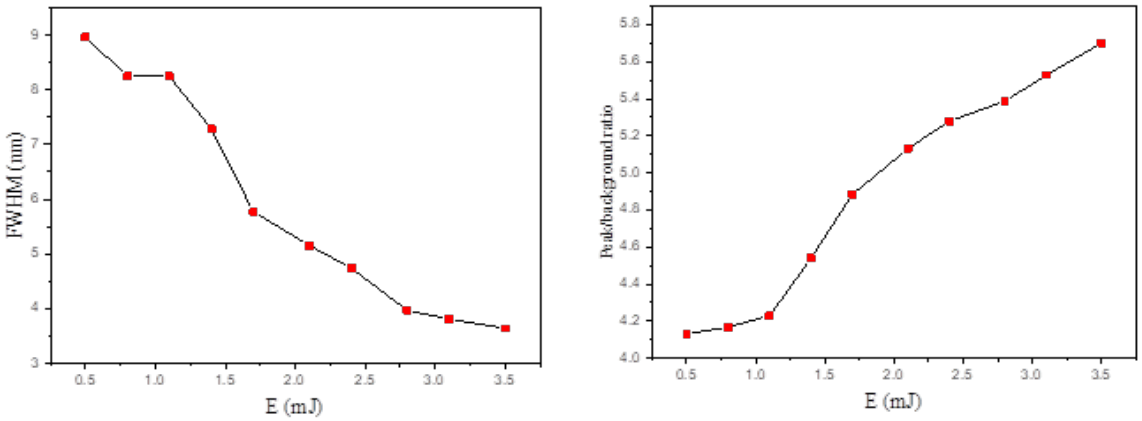


Fig.7. (a) Extracted FWHM as a function of pump energy and (b) Peak-to-background ratio as a function of pump energy.

CC BY

measured peak intensity reached 25,458.833 a.u., with a full width at half maximum (FWHM) of 5.771 nm. Beyond this threshold, the emission intensity continued to increase, accompanied by changes in the spectral linewidth and peak-to-background ratio. In particular, at a pump energy of 3.5 mJ, the FWHM decreased to 3.641 nm, while the peak-to-background ratio increased to 5.700. These spectral changes suggest enhanced optical amplification and improved spectral definition of the random-laser emission at higher pump energies. Accordingly, the random-lasing threshold of the Ag-nanowire/R6G structure under the present experimental conditions was

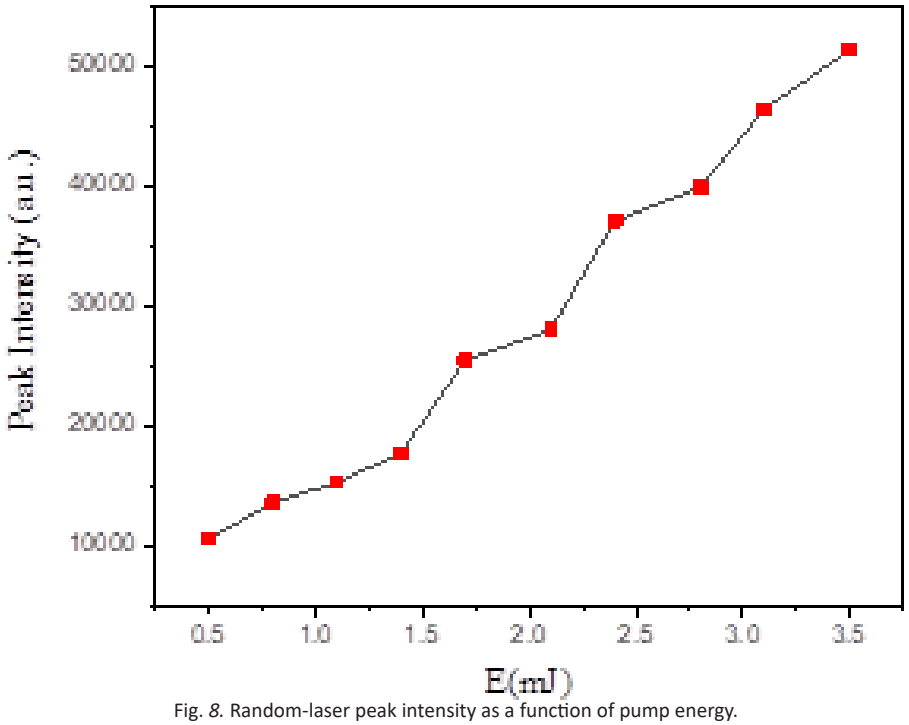


Fig. *8.* Random-laser peak intensity as a function of pump energy.

Table 4. Summary of principal random-laser findings.

Parameter	Result	Interpretation
Peak intensity	10,610 → 51,353 a.u.	4.84× increase from 0.5 to 3.5 mJ
Peak wavelength	566.31–566.58 nm	Maximum shift ≈0.27 nm
Minimum analyzed FWHM	≈3.641 nm	At 3.5 mJ
Maximum peak/background	≈5.70	At 3.5 mJ
Lasing threshold	1.7 mJ	Calculated from pump-energy-dependent emission response

CC BY

estimated to be approximately 1.7 mJ (Table 4).

CONCLUSION

A silver-nanowire-assisted R6G plasmonic random-laser system was experimentally investigated through gain-medium optimization and pump-energy-dependent emission measurements. The absorption of R6G increased with concentration, whereas the fluorescence intensity reached its maximum at 1×10^{-5} M, indicating that this concentration was the most suitable gain medium among the investigated samples. Using the optimized R6G concentration in the Ag-nanowire-based multilayer structure, an increase in pump energy from 0.5 to 3.5 mJ resulted in an increase in emission peak intensity from 10,610.167 to 51,353.000 a.u., corresponding to an approximately 4.84-fold enhancement. The emission wavelength remained highly stable over the range of 566.308–566.577 nm, with a maximum shift of only approximately 0.27 nm. The spectral linewidth exhibited pronounced narrowing, with the full width at half maximum (FWHM) decreasing from 8.958 nm at 0.5 mJ to 3.641 nm at 3.5 mJ. In parallel, the peak-to-background ratio increased from 4.163 to 5.700, indicating an increasingly well-defined emission feature relative to the spectral background at higher pump energies. Based on the pump-energy-dependent emission behavior, the lasing threshold was calculated to be 1.7 mJ. Above this threshold, the increase in emission intensity, together with spectral narrowing and enhanced peak-to-background contrast, indicates a transition toward a more pronounced stimulated-emission regime. These combined characteristics support the occurrence of pump-dependent random-laser emission in the investigated hybrid gain–scattering system. The results are consistent with a distributed-feedback mechanism in which R6G provides optical gain, while the Ag nanowire network provides multiple scattering pathways and plasmon-mediated optical interactions. The obtained threshold of 1.7 mJ provides a quantitative characteristic of the investigated structure and establishes the pump-energy level at which random-laser emission becomes pronounced.

CONFLICT OF INTEREST

The authors declare that there is no conflict of interests regarding the publication of this manuscript.

REFERENCES

1. Jawad MK, Jassim JM, Haddawi SF, Hamidi SM. Signature of light localization and temperature enhancement on core-shell-based plasmonic random laser. Nano-Structures and Nano-Objects. 2025;44:101567.
2. Li S, Wang L, Zhai T, Xu Z, Wang Y, Wang J, et al. Plasmonic random laser on the fiber facet. Opt Express. 2015;23(18):23985.
3. Zhai T, Chen J, Chen L, Wang J, Wang L, Liu D, et al. A plasmonic random laser tunable through stretching silver nanowires embedded in a flexible substrate. Nanoscale. 2015;7(6):2235-2240.
4. Haddawi SF, Mirahmadi M, Mbarak H, Kodeary AK, Ghasemi M, Hamidi SM. Footprint of plexcitonic states in low-power green–blue plasmonic random laser. Appl Phys A. 2019;125(12).
5. Haddawi SF, Humud HR, Hamidi SM. Signature of plasmonic nanoparticles in multi-wavelength low power random lasing. Optics and Laser Technology. 2020;121:105770.
6. Haddawi SF, Kodeary AK, Shnan NS, Roostaei N, Hamidi SM, Humud HR. Vertically emitted dual wavelength random laser based on light emitting polymers and silver nanowires double cavity structure. Optik. 2020;219:165256.
7. Ejbarah RA, Jassim JM, Haddawi SF, Hamidi SM. Transition from incoherent to coherent random lasing by adjusting silver nanowires. Appl Phys A. 2021;127(6).
8. Haddawi SF, Humud HR, Monfared SA, Hamidi SM. Two-dimensional plasmonic multilayer as an efficient tool for low power random lasing applications. Waves in Random and Complex Media. 2021;34(3):1640-1649.
9. Gayathri R, Suchand Sandeep CS, Gummaluri VS, Asik RM, Padmanabhan P, Gulyás B, et al. Plasmonic random laser enabled artefact-free wide-field fluorescence bioimaging: uncovering finer cellular features. Nanoscale Advances. 2022;4(10):2278-2287.
10. Lawandy NM, Balachandran RM, Gomes ASL, Sauvain E. Laser action in strongly scattering media. Nature. 1994;368(6470):436-438.
11. Wiersma DS, van Albada MP, Lagendijk A. Random laser? Nature. 1995;373(6511):203-204.
12. Wiersma DS, Lagendijk A. Light diffusion with gain and random lasers. Physical Review E. 1996;54(4):4256-4265.
13. Cao H, Xu JY, Chang SH, Ho ST. Transition from amplified spontaneous emission to laser action in strongly scattering media. Physical Review E. 2000;61(2):1985-1989.
14. Cao H, Xu JY, Zhang DZ, Chang SH, Ho ST, Seelig EW, et al. Spatial Confinement of Laser Light in Active Random Media. Phys Rev Lett. 2000;84(24):5584-5587.
15. Cao H. Lasing in random media. Waves in Random Media. 2003;13(3):R1-R39.
16. Cao H. Review on latest developments in random lasers with coherent feedback. J Phys A: Math Gen. 2005;38(49):10497-10535.
17. Cao H. Random Lasers: Development, Features and Applications. Optics and Photonics News. 2005;16(1):24.
18. Wiersma DS. The physics and applications of random lasers. Nature Physics. 2008;4(5):359-367.
19. Fallert J, Dietz RJB, Sartor J, Schneider D, Klingshirn C, Kalt H. Co-existence of strongly and weakly localized random laser modes. Nature Photonics. 2009;3(5):279-282.
20. van der Molen KL, Tjerkstra RW, Mosk AP, Lagendijk A. Spatial Extent of Random Laser Modes. Phys Rev Lett.

CC BY

2007;98(14).
21. Luan F, Gu B, Gomes ASL, Yong K-T, Wen S, Prasad PN. Lasing in nanocomposite random media. Nano Today. 2015;10(2):168-192.
22. Gomes ASL, Moura AL, de Araújo CB, Raposo EP. Recent advances and applications of random lasers and random fiber lasers. Progress in Quantum Electronics. 2021;78:100343.
23. Sun Y. Silver nanowires – unique templates for functional nanostructures. Nanoscale. 2010;2(9):1626.
24. Xiong X, Zou CL, Ren XF, Liu AP, Ye YX, Sun FW, et al. Silver nanowires for photonics applications. Laser and Photonics Reviews. 2013;7(6):901-919.
25. Pyayt AL, Wiley B, Xia Y, Chen A, Dalton L. Integration of photonic and silver nanowire plasmonic waveguides. Nature Nanotechnology. 2008;3(11):660-665.
26. Wang Z, Wei H, Pan D, Xu H. Controlling the radiation direction of propagating surface plasmons on silver nanowires. Laser and Photonics Reviews. 2014;8(4):596-601.
27. Zhang D, Xiang Y, Chen J, Cheng J, Zhu L, Wang R, et al. Extending the Propagation Distance of a Silver Nanowire Plasmonic Waveguide with a Dielectric Multilayer Substrate. Nano Lett. 2018;18(2):1152-1158.
28. Würth C, González MG, Niessner R, Panne U, Haisch C, Genger UR. Determination of the absolute fluorescence quantum yield of rhodamine 6G with optical and photoacoustic methods – Providing the basis for fluorescence quantum yield standards. Talanta. 2012;90:30-37.
29. Arbeloa FLp, Ojeda PR, Arbeloa IiLp. Dimerization and trimerization of rhodamine 6G in aqueous solution. Effect on the fluorescence quantum yield. Journal of the Chemical Society, Faraday Transactions 2. 1988;84(12):1903.
30. Chang S-H, Wu J-J, Kuo C-C, Tsay S-Y, Chen Y-H, Lin J-H. Plasmonic random laser from dye-doped cholesteric liquid crystals incorporating silver nanoprisms. Opt Lett. 2020;45(18):5144.
31. Schokker AH, Koenderink AF. Lasing at the band edges of plasmonic lattices. Physical Review B. 2014;90(15).
32. Lateef M, Aldaim WA, Haddawi SF, Hamidi SM. Mouse Tissue imaging by random laser of Plasmonic two dimensional array. Springer Science and Business Media LLC; 2024. http://dx.doi.org/10.21203/rs.3.rs-4921013/v1
33. Sun Y, Wang Z, Shi X, Wang Y, Zhao X, Chen S, et al. Coherent plasmonic random laser pumped by nanosecond pulses far from the resonance peak of silver nanowires. J Opt Soc Am B. 2013;30(9):2523.
34. Abdulameer ND, Shnan NS, Aboud LH, Hamidi SM. Laser induced fluorescence enhancement by surface lattice resonance in two dimensional plasmonic nanostructure. Appl Phys A. 2025;131(6).
35. Haddawi M, Jasim J, Hamidi SM. Magneto-Plasmonic-Induced Random Laser in Two-Dimensional Feb Square Array. Elsevier BV; 2023. http://dx.doi.org/10.2139/ssrn.4401722

CC BY